Energy Structure of a Finite Haldane Chain in $Y_2BaNi_{0.96}Mg_{0.04}O_5$ Studied by High Field Electron Spin Resonance

M. Yoshida,[1] K. Shiraki,[2] S. Okubo,[1,3] H. Ohta,[1,3] T. Ito,[4] H. Takagi,[4,5] M. Kaburagi,[6] and Y. Ajiro[7]

[1]*Venture Business Laboratory, Kobe University, Kobe 657-8501, Japan*
[2]*The Graduate School of Science and Technology, Kobe University, Kobe 657-8501, Japan*
[3]*Molecular Photoscience Research Center, Kobe University, Kobe 657-8501, Japan*
[4]*CERC, National Institute of Advanced Industrial Science and Technology, Tukuba, Ibaraki 305-8562, Japan*
[5]*Graduate School of Frontier Sciences, The University of Tokyo, Kashiwa, Chiba 277-8561, Japan*
[6]*Faculty of Cross-Cultural Studies, Kobe University, Kobe 657-8501, Japan*
[7]*Department of Chemistry, Kyoto University, Kyoto 606-8502, Japan*

(Received 14 January 2005; published 7 September 2005)

This Letter presents the fine structure of energy levels for the edge states of a Haldane chain. In order to investigate the edge states, we have performed high field and multifrequency electron spin resonance (ESR) measurements of finite length $S = 1$ antiferromagnetic chains in $Y_2BaNi_{0.96}Mg_{0.04}O_5$. Owing to the high spectral resolution by high fields and high frequencies, observed ESR signals can be separated into the contributions of the finite chains with various chain lengths. Our results clearly show that the edge spins actually interact with each other through the quantum spin chain and the interaction depends on the chain length N. This N dependence has been obtained experimentally for the first time, and shows that the correlation length ξ in the real system is somewhat larger than that calculated by a simple Heisenberg model.

DOI: 10.1103/PhysRevLett.95.117202 PACS numbers: 75.50.Ee, 75.10.Jm, 76.30.−v

Low dimensional quantum spin systems often have disordered spin liquid states due to quantum fluctuations. Such a spin liquid state is coherent over the macroscopic length scale, while the state differs from a classical ordered state. One dimensional (1D) antiferromagnetic (AFM) spin systems with $S = 1$ have attracted much attention, since Haldane conjectured that a 1D AFM Heisenberg chain with integer spin would have an energy gap between the ground state and the first excited state [1]. The Haldane system belongs to such quantum spin systems and has a unique ground state. The ground state of a Haldane chain can be well described by the Affleck-Kennedy-Leib-Tasaki model [2]. In this model, the $S = 1$ states are described as two $S = 1/2$ states and the ground state corresponds to a valence-bond-solid state where each $S = 1/2$ forms a singlet with the nearest neighbor belonging to the adjacent site. If the chain is broken (i.e., open boundary conditions), two effective $S = 1/2$ spins are created, one at each end of the finite chain [3]. The direct experimental evidence of the existence of such effective $S = 1/2$ spins was given by the electron spin resonance (ESR) on $Ni(C_2H_8N_2)_2NO_2(ClO_4)$ containing magnetic or nonmagnetic impurities [4–6].

Y_2BaNiO_5, which has an orthorhombic structure with lattice parameters $a = 3.76$, $b = 5.76$, and $c = 11.32$ Å [7], is known as a model substance for the Haldane system, and the Ni^{2+} chains run along the a axis. The intrachain exchange interaction J and the Haldane gap have been estimated to be about 280 and 100 K, respectively, from the magnetic susceptibility and the inelastic neutron scattering measurements [8–12]. The single-ion anisotropy parameters $|D| \sim 0.039J$ and $|E| \sim 0.0127J$ were also evaluated from the neutron scattering measurements [11,12]. In this compound, the presence of $S = 1/2$ states has been tested by studying specific heat and ESR of defects [13–16]. And the results of the specific heat and K-band (24 GHz) ESR measurements for doping with nonmagnetic impurities have been explained by the finite chain model [15,16]. In this model, the substitution of nonmagnetic ions for Ni provides a simple break in the chain, and then produces an ensemble of finite length chain segments. When the chain length N is sufficiently larger than the correlation length ξ for the Haldane chain, the effective $S = 1/2$ spins at the chain ends are nearly free. However, when N is comparable to 2ξ, the interaction between them is considerable. This interaction produces a ferromagnetic dimer for odd N or an AFM dimer for even N. Batista *et al.* introduced the low-energy effective Hamiltonian

$$H_{\mathrm{eff}} = E_0(N) + [J\alpha(N) + D\beta(N)]|0\rangle\langle 0| + D\gamma(N)S_z^2 + E\gamma(N)\{S_x^2 - S_y^2\} - \mu_B \sum_{\mu\nu} B^\mu g^{\mu\nu} S^\nu, \tag{1}$$

where $E_0(N)$, $\alpha(N)$, $\beta(N)$, and $\gamma(N)$ are functions of N, x, y, and z correspond to the b, c, and a axes, $\mathbf{S}$ is the spin operator for the dimer, $|0\rangle$ is the singlet state, and $g^{\mu\nu}$ is the gyromagnetic tensor [16]. They computed the functions of N by using the density-matrix renormalization group (DMRG) technique with $E = 0$, and then they showed that the main peak and characteristic secondary peaks appear in ESR spectra [16]. However, the experimental results are not convincing at all to support their finite chain model. The ESR measurement was done only at K band and only 4 secondary peaks were observed. Furthermore, the agreement between experiment and theory was not satisfactory. Secondary peaks can appear for other reasons such as crystal defects [13], interaction through the impurity site, or magnetic impurities. Therefore, it is necessary to verify that the secondary peaks originate from the finite chains by measuring the frequency dependence of the signals. In addition, N for the observed secondary peaks and the parameters D, E, and γ were not determined. It is also important to obtain parameters experimentally and compare them with calculations.

Recently, impurity-induced edge states have been studied intensively by microscopic measurements such as neutron scattering and NMR [17–20], because these states reflect the underlying features of the quantum spin systems. The interaction between edge spins and the N dependence of the energy states predicted by the Hamiltonian (1) are directly related to the spin liquid nature of the Haldane system. Therefore, it is of interest to study the energy states for a finite chain and their N dependence. Although the result of the inelastic neutron scattering measurements for the edge spins was explained by the finite chain model consistently [19], the neutron scattering measurements did not show direct evidence for N dependence, because the measurements could not separate the contributions of individual finite chains. In this Letter, we present the fine structure of energy levels for the impurity-induced edge states in the 1D $S = 1$ Heisenberg antiferromagnet $Y_2BaNi_{0.96}Mg_{0.04}O_5$ obtained through high field and multifrequency ESR measurements. Owing to the high spectral resolution by high fields and high frequencies [21], observed ESR signals are well separated into the contributions of the N-length chains. Our ESR results show that the edge spins for a finite Haldane chain in $Y_2BaNi_{0.96}Mg_{0.04}O_5$ actually interact with each other through the finite chain and the interaction depends on the chain length N. And then, we determine the effective single-ion anisotropy parameters $D\gamma(N)$ and $E\gamma(N)$ from $N = 1$ to 27 precisely. The N dependence of the energy states of the edge spins contains direct and precise information about ξ.

High field ESR measurements of the single crystal of $Y_2BaNi_{0.96}Mg_{0.04}O_5$ have been performed in the temperature range from 4.2 to 80 K using the pulsed magnetic field up to 15 T. The details of our experimental setups can be found in Refs. [21–24]. The samples were grown by the traveling-solvent floating-zone method [25]. The size of the single crystal used in our experiment is about $3 \times 4 \times 5$ mm^3.

Figure 1 shows the ESR spectra for various frequencies at 4.2 K in the magnetic field B parallel to the c axis. A prominent absorption line is observed at the slightly lower field side of the 1,1-diphenyl-2-picrylhydrazyl (DPPH) marker at each frequency. In addition, many small secondary peaks are observed all over the spectra. Such main peak and some secondary peaks are reported in Ref. [16]. In the previous report, however, the ESR measurements were performed only at K band, and there was no direct evidence that observed secondary peaks really originated from the edge spins of the finite chains because observed secondary peaks are limited. In our measurements with the high field and high frequencies, the secondary peaks are observed very clearly and are separable from each other. Furthermore, the frequency dependence can be discussed in our measurements. Frequency dependence measurements are essential for determining the origin of ESR signals. From these results, as shown later, the main peak and secondary peaks can be assigned to the contributions of large N chains and small odd N chains, respectively. For example, the contributions of N-length chains are labeled $N(= 1, 3, 5, 7)$ for 210 GHz in Fig. 1. Similar measurements were also performed for $B \parallel a$ and $B \parallel b$, where the prominent main peak and small secondary peaks were also observed.

Figure 2 shows the frequency-field diagrams for the a, b, and c axes. These diagrams are obtained by taking into account all separable peaks in observed spectra. The resonance points for the main peak are on the straight lines that cross the origin. The main peak should correspond to the effective $S = 1/2$ spins at the chain ends for large N chains, because the resonance mode for the main peak has no influence of D and E terms. From the slopes of the dashed lines, g^{aa}, g^{bb}, and g^{cc} values are estimated to be 2.25, 2,18, and 2.16, respectively. These values of the main peak are quite consistent with those in Ref. [16]. On the other hand, the resonance points for secondary peaks are well explained by the Hamiltonian (1). Here, as an even chain has a singlet ground state $|0\rangle$, which has the energy $J\alpha + D\beta(\alpha, \beta < 0)$, the signals for the transitions between the triplets of even chains decrease with decreasing temperature. Therefore, ESR signals from odd chains are dominant at low temperatures. According to the Hamiltonian (1), an odd chain is described as an $S = 1$

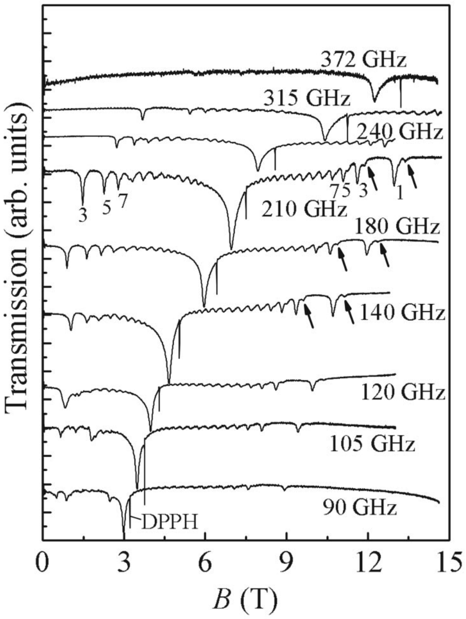

FIG. 1. ESR spectra for various frequencies at 4.2 K in the magnetic field B parallel to the c axis.

spin with effective single-ion anisotropy parameters $D\gamma$ and $E\gamma$. The energy levels for such an $S = 1$ spin in the magnetic field are shown in Fig. 3. There are three possible ESR transitions for each direction and they are labeled as a_i, b_i, and c_i ($i = 1, 2$, and 3). In general, the transitions a_3, b_3, and c_3 are forbidden. In the present case, however, the transitions a_3, b_3, and c_3 are possible due to the mixing between the $|11\rangle$, $|10\rangle$, and $|1-1\rangle$ states through $D\gamma$ and $E\gamma$. In Fig. 2, the thick solid lines are calculated with $D\gamma = -8.97$ K, $E\gamma = -2.98$ K, and the g^{aa}, g^{bb}, and g^{cc} values obtained above, and are labeled as a_i, b_i, and c_i corresponding to those in Fig. 3. As shown in Fig. 2, these thick lines form the set of the resonance modes that corresponds to the resonance for the $S = 1$ spin with the largest $|D\gamma|$ and $|E\gamma|$ values. Here, the DMRG calculation showed that $\gamma(N)$ decreases with increasing N [16]. Therefore, the $S = 1$ spin with the largest $|D\gamma|$ and $|E\gamma|$ corresponds to the chain with $N = 1$, that is, the single Ni spin lying between Mg impurities. The consistency between the anisotropy parameters obtained in our measurements and those obtained in Y_2BaNiO_5 [11,12] is very good. We believe that the signals with $D\gamma = -8.97$ K and $E\gamma = -2.98$ K correspond to $N = 1$, because the $D\gamma$ and $E\gamma$ are close to the anisotropy parameters in Y_2BaNiO_5, and we could not find signals with more large $|D\gamma|$ and $|E\gamma|$ values in the measurements of the frequency region up to 420 GHz.

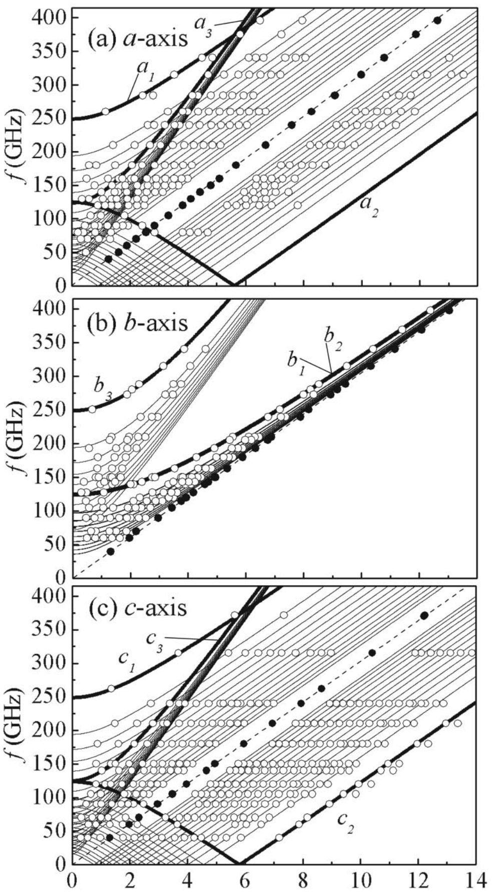

FIG. 2. Frequency-field diagrams for the applied field B along different directions (a) $B \parallel a$, (b) $B \parallel b$, and (c) $B \parallel c$. The solid and open circles represent the resonance points for the main peak and secondary peaks, respectively. The dashed lines indicate the resonance modes for free $S = 1/2$ spins.

As shown in Fig. 2, the data of all other secondary peaks can also be indicated by the thin solid lines. These lines are calculated with various $D\gamma$ and $E\gamma$, which are in the ranges of -1.08 to -7.00 K and -0.36 to -2.32 K, respectively. Because $\gamma(N)$ is expected to decrease with increasing N and to approach zero, the resonance modes should approach the gapless mode as increasing N. Here, the gapless mode corresponds to that of the main peak, which is considered to be due to free $S = 1/2$ spins at the chain ends for large N chains. From these fittings shown in Fig. 2, it is clear that the low-energy edge states for the Haldane chain in $Y_2BaNi_{0.96}Mg_{0.04}O_5$ are well described by the Hamiltonian (1). As a result, we obtain the single-ion anisotropy parameters as a function of N. Here, it should be noted that the fitting parameter is only $\gamma(N)$. Figure 4 shows the obtained $\gamma(N)$ values. In our measurements, $\gamma(N)$ are evaluated up to $N = 27$. For $N \geq 29$, absorption lines are difficult to distinguish from each other due to the limit of our experimental resolution, and they contribute to the main peak as large N chains. The $\gamma(N)$ values obtained by our experiments are compared with those calculated from the DMRG method with $E = 0$ [16]. As shown in Fig. 4, the N dependence of $\gamma(N)$ obtained experimentally is qualitatively consistent with that obtained by the calculation. However, there is a small disagreement; that is, the experimental $\gamma(N)$ value is somewhat larger than the calculation value for large N. This result shows that the correlation length ξ in the real system is somewhat larger than that in the model used in Ref. [16]. In the pure Heisenberg model, ξ is estimated to be about 6 [3,26–28]. The precise ξ value can be obtained from our result by

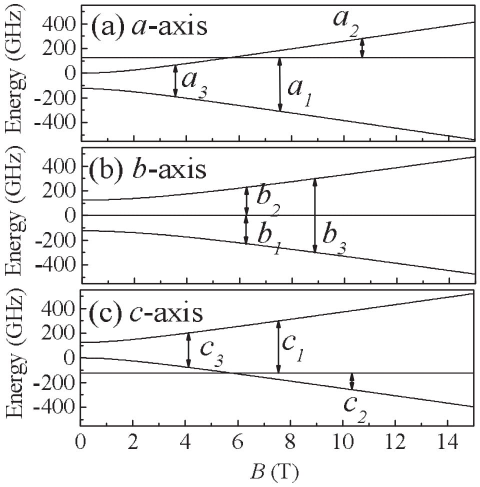

FIG. 3. Energy levels for a $S = 1$ spin with $D = -8.97$ and $E = -2.98$ K in the applied field B along different directions (a) $B \parallel a$, (b) $B \parallel b$, and (c) $B \parallel c$.

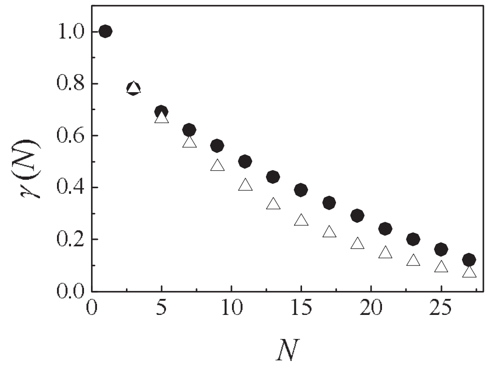

FIG. 4. N dependence of $\gamma(N)$. The solid circles and open triangles represent $\gamma(N)$ obtained by our experiment and calculated in Ref. [16], respectively.

comparison with a more sophisticated model, but this is a future problem.

In the above analysis, we consider only the odd chains. However, the same number of the even chains exists in the system. The edge spins are considered to be free $S = 1/2$ spins in large even N as well as large odd N, because the singlet gap is also expected to decrease rapidly and to approach zero with increasing N. In this region, we cannot distinguish between contributions of odd and even chains to the spectrum. For $N = 2$ and 4, the singlet gap $J\alpha + D\beta$ is very large due to the large $J(= 280\text{ K})$, so that at low temperatures we cannot observe the even chain signals corresponding to the chains of $N = 2$ and 4. For $6 \leq N \leq 10$, we can observe the signals coming from the excited triplet by increasing the temperature above 4.2 K. The temperature dependence of these signals can be explained by considering the singlet gap $J\alpha + D\beta$ calculated in Ref. [16]. For $12 \leq N$, the signals can be visible in the spectra at 4.2 K, because the singlet gap is comparable with 4.2 K. However, these signals of even chains are still weaker than those of odd chains. In this situation, the signals for odd chains overlap with the signals for even chains. Consequently, it is difficult to specify the signals for even chains clearly. It should be noted that some additional peaks, which are indicated by arrows in Fig. 1, are observed. A crystal of Y_2BaNiO_5 often has a mosaic structure due to small tilts of c axes. Therefore, these signals originate from a small domain whose c axis slightly tilts from that for the main part of the sample.

It should also be noted that the signal intensity decreases with increasing N for the odd chains as shown in Fig. 1. Assuming the random distribution of Mg, the proportion of the N length chain is proportional to 0.96^N. Therefore, the decrease of the intensity is due to the distribution probability. However, the excited levels also affect the intensity, if the energy separation between an excited level and the ground state is comparable to the temperature. Furthermore, the ESR transition probability should also depend on N. Consequently, the N dependence of the integrated intensity cannot be explained by a simple model.

In summary, we have performed high field and multifrequency ESR measurements of finite length $S = 1$ AFM chains in $Y_2BaNi_{0.96}Mg_{0.04}O_5$. By using the high field and high frequencies, we have succeeded in observing the ESR signals from finite chains with various chain lengths separately. And then, we determined $D\gamma$ and $E\gamma$ for each odd N. The N dependence of $D\gamma$ and $E\gamma$ provides direct information about the correlation length ξ and shows that ξ in the real system is somewhat larger than that calculated by a simple Heisenberg model. A more sophisticated model is necessary for explaining the experimental result.

This work was supported by a Grant-in-Aid for Science Research on Priority Areas (B) (No. 13130204 "Field-Induced New Quantum Phenomena in Magnetic Systems") from the Ministry of Education, Culture, Sports, Science and Technology of Japan. The authors M. Y., S. O., and H. O. are grateful for the financial support from the Venture Business Laboratory of Kobe University.

[1] F. D. Haldane, Phys. Rev. Lett. **50**, 1153 (1983).
[2] I. Affleck *et al.*, Phys. Rev. Lett. **59**, 799 (1987).
[3] T. Kennedy, J. Phys. Condens. Matter **2**, 5373 (1990).
[4] M. Hagiwara *et al.*, Phys. Rev. Lett. **65**, 3181 (1990).
[5] S. H. Glarum *et al.*, Phys. Rev. Lett. **67**, 1614 (1991).
[6] Y. Ajiro *et al.*, J. Phys. Soc. Jpn. **66**, 971 (1997).
[7] D. J. Buttrey, J. D. Sullivan, and A. L. Reigold, J. Solid State Chem. **88**, 291 (1990).
[8] J. Darriet and L. P. Regnault, Solid State Commun. **86**, 409 (1993).
[9] B. Batlogg, S.-W. Cheong, and J. L. W. Rupp, Physica (Amsterdam) **194–196B**, 173 (1994).
[10] T. Yokoo *et al.*, J. Phys. Soc. Jpn. **64**, 3651 (1995).
[11] Y. Sakaguchi *et al.*, J. Phys. Soc. Jpn. **65**, 3025 (1996).
[12] G. Xu *et al.*, Phys. Rev. B **54**, R6827 (1996).
[13] S. Kimura *et al.*, J. Phys. Soc. Jpn. **67**, 2514 (1998).
[14] A. P. Ramirez, S.-W. Cheong, and M. L. Kaplan, Phys. Rev. Lett. **72**, 3108 (1994).
[15] C. D. Batista, K. Hallberg, and A. A. Aligia, Phys. Rev. B **58**, 9248 (1998).
[16] C. D. Batista, K. Hallberg, and A. A. Aligia, Phys. Rev. B **60**, R12 553 (1999).
[17] F. Tedoldi, R. Santachiara, and M. Horvatíc, Phys. Rev. Lett. **83**, 412 (1999).
[18] G. Xu *et al.*, Science **289**, 419 (2000).
[19] M. Kenzelmann *et al.*, Phys. Rev. Lett. **90**, 087202 (2003).
[20] J. Das *et al.*, Phys. Rev. B **69**, 144404 (2004).
[21] H. Ohta *et al.*, J. Phys. Soc. Jpn. Suppl. B **72**, 26 (2003).
[22] M. Motokawa, H. Ohta, and N. Makita, Int. J. Infrared Millim. Waves **12**, 149 (1991).
[23] S. Kimura *et al.*, Int. J. Infrared Millim. Waves **17**, 833 (1996).
[24] N. Nakagawa *et al.*, Int. J. Infrared Millim. Waves **19**, 167 (1998).
[25] T. Ito *et al.*, Phys. Rev. B **64**, 060401 (2001).
[26] S. Miyashita and S. Yamamoto, Phys. Rev. B **48**, 913 (1993).
[27] S. R. White, Phys. Rev. Lett. **69**, 2863 (1992).
[28] S. R. White and D. A. Huse, Phys. Rev. B **48**, 3844 (1993).